View metadata, citation and similar papers at core.ac.uk
brought to you by CORE
provided by Apollo

14th European Conference on Applied Superconductivity (EUCAS 2019) IOP Publishing
Journal of Physics: Conference Series **1559** (2020) 012027 doi:10.1088/1742-6596/1559/1/012027

# Simulation of mechanical stresses in reinforced REBaCuO ring bulks during pulsed-field magnetization

**T. Hirano[1], H. Fujishiro[1], T. Naito[1] and M. D. Ainslie[2]**

[1] Department of Physical Science and Materials Engineering, Faculty of Science and Engineering, Iwate University, 4-3-5 Ueda Morioka, Japan
[2] Bulk Superconductivity Group, Department of Engineering, University of Cambridge, Trumpington Street, Cambridge CB2 1PZ, UK

E-mail: g0318132@iwate-u.ac.jp

**Abstract**. We have performed numerical simulations of the electromagnetic, thermal and mechanical properties of a REBaCuO ring-shaped bulk with various reinforcement structures during pulsed-field magnetization (PFM). Compressive and tensile electromagnetic stresses, $\sigma_\theta^{mag}$, are developed in the ring-shaped bulk during the ascending and descending stages of PFM, respectively. These stresses increase at lower operating temperatures and for higher applied pulsed fields. In order to reduce these stresses, the ring-shaped bulk was fully encapsulated by outer and inner ring with upper and lower plates made by Al alloy. In particular, this reinforcement structure can achieve the lowest electromagnetic compressive stress, which corresponds to about 54% of that for a conventional ring reinforcement structure, and the electromagnetic tensile stress was also reduced. We also compared the simulation results of the electromagnetic stresses for the ring-shaped bulk to those for a disk-shaped bulk.

## 1. Introduction

REBaCuO (RE: rare earth element or Y) superconducting bulks have promising potential to trap magnetic fields of over 20 T. As a result, such bulks have been used as strong trapped-field magnets (TFMs) in practical applications such as a compact cryogen-free nuclear magnetic resonance (NMR) spectrometer [1] and rotating machines [2]. However, TFMs suffer from mechanical fracture due to a large Lorentz force, $\boldsymbol{F} = \boldsymbol{J} \times \boldsymbol{B}$ ($\boldsymbol{J}$ represents the current density and $\boldsymbol{B}$ represents the magnetic field), that is generated during field-cooled magnetization (FCM) from higher applied magnetic fields, in which only an electromagnetic tensile stress develops in the bulk [3]. We have investigated the mechanical properties of REBaCuO disk- and ring-shaped bulks during FCM using numerical simulations and proposed an optimal reinforcement structure by metal to prevent mechanical fracture [4 - 8]. On the other hand, the pulsed-field magnetization (PFM) process consists of an ascending (flux penetration) stage on the order of milliseconds and a descending (flux flow) stage, during which electromagnetic compressive (ascending stage) and tensile (descending stage) stresses are developed in the bulk [9, 10]. Accordingly, the optimal reinforcement structure for PFM, which may be different from that for FCM, may need to be considered. As for a shape of the bulk, the risk of fracture for the ring-shaped bulk is higher than that of the disk-shaped bulk due to the stress concentration at the inner edge of the concentric hole [11]. The mechanical properties have been also investigated analytically for disk- and ring-shaped bulks with infinite height during FCM and zero-field-cooled magnetization (ZFCM) [11 - 13]. In

Content from this work may be used under the terms of the Creative Commons Attribution 3.0 licence. Any further distribution of this work must maintain attribution to the author(s) and the title of the work, journal citation and DOI.
Published under licence by IOP Publishing Ltd

addition, numerical simulations of the mechanical stresses have been performed using finite element method (FEM) for disk-shaped bulks during PFM [9, 10, 14]. The final trapped field of the ring-shaped bulk during PFM experiment, which was negative value at the centre of the bulk, has been reported in previous studies [15]. In order to realize the higher TFMs in ring-shaped bulk by PFM, in this study, we investigate the mechanical and thermal stresses during PFM for REBaCuO ring bulks using numerical simulations and proposed an effective reinforcement structure. We also compare the mechanical stress for the ring-shaped bulk to that for the disk-shaped bulk.

## 2. Numerical simulation Procedure

Based on our experimental setup for PFM [15], we constructed a three-dimensional model for a REBaCuO ring-shaped bulk (60 mm in outer diameter (O.D.), 36 mm in inner diameter (I.D.) and 17 mm in height (H)), as shown in Fig. 1(a). The ring-shaped bulk was mounted in an Al alloy ring holder (70 mm in O.D. and 60 mm in I.D.) with the same height as the bulk. The Al alloy is a suitable material for the reinforcement of the ring-shaped bulk for NMR apparatus because it is non-magnetic and has higher mechanical strength, compared to pure aluminum. The bulk was cooled to $T_s$ = 65, 45 and 25 K from the bottom surface, and was magnetized by PFM using a solenoid coil (120 mm in O.D., 100 mm in I.D. and 50 mm in H). A single magnetic pulse with a rise time of 13 ms and a duration time of 150 ms, and amplitudes ranging from $B_{ex}$ = 1.0 to 4.5 T, was applied to the bulk via a pulsed current in the coil. The time evolution of trapped magnetic field, $B_t(t)$, was monitored at the centre of the ring-shaped bulk ($r = z = 0$ mm). Physical phenomena during PFM are described by the fundamental electromagnetic and thermal equations in [16]. The power-$n$ law ($n$ = 20) was used to describe the highly nonlinear $E$-$J$ characteristic of the bulk material [17]. The following magnetic field and temperature dependence of critical current density, $J_c(B, T)$, proposed by Kim [18], was used in the simulation.

$$J_c(B,T) = \alpha \left\{1 - \left(\frac{T}{T_c}\right)^2\right\}^{\frac{3}{2}} \frac{B_0}{|B|+B_0}, \qquad (1)$$

where $T_c$ = 92 K is the transition temperature of the REBaCuO bulk, and $B_0$ = 1.3 T and $\alpha = 3.45 \times 10^9$ A/m$^2$ were assumed. The REBaCuO bulk is assumed to be isotropic and homogeneous for simplicity. The commercial software package, Photo-Eddy, combined with Photo-Thermo and Photo-Elas (Photon Ltd, Japan), were used for analyses of electromagnetic, thermal and mechanical properties. The numerical simulation procedure and the parameters used in the simulation were described elsewhere in detail [16]. Elastic behaviour of an isotropic material can be explained by Hooke's law, in which the stress is linearly proportional to the strain [4]. The electromagnetic hoop stress, $\sigma_\theta^{mag}$, and the thermal hoop stress, $\sigma_\theta^{therm}$, were calculated for each case during PFM. Table 1 summarizes the assumed mechanical parameters (Young's modulus, $E$, Poisson ratio, $\nu$, and thermal expansion coefficient, $\alpha_0$) of the REBaCuO bulk and the Al alloy.

The $\sigma_\theta^{mag}$ and $\sigma_\theta^{therm}$ values for the bulk reinforced by a simple Al alloy ring, denoted as "Ring", in Fig. 1(a), were compared to those for the bulks with various reinforcement structures. An Al alloy inner ring of 5 mm in width and an upper Al alloy plate 2 mm in thickness were added to the "Ring" setup, as shown in Fig. 1(b). We denote this setup as "Cap Cover". The ring-shaped bulk with the "Cap Cover" was further reinforced by a lower Al alloy plate 2 mm in thickness, as shown in Fig. 1(c). We denote this setup as "Full Cover". The width of the inner ring for the "Full Cover" was increased from 5 mm to 9 mm, as shown in Fig. 1(d). We abbreviate this setup as "Full Cover wide".

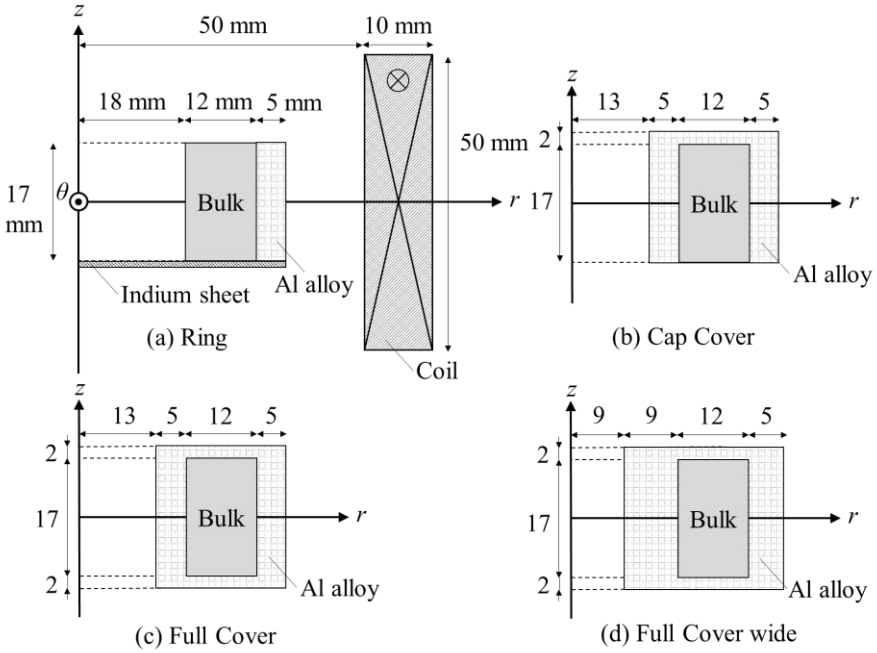


**Figure 1**. Schematic view of the numerical models of the various reinforcement structures for the ring-shaped bulk: (a) "Ring", (b) "Cap Cover", (c) "Full Cover" and (d) "Full Cover wide".

**Table 1**. Mechanical parameters of REBaCuO bulk and Al alloy used in the simulation.

| | $E$ (GPa) | $\nu$ | $\alpha_0$ ($K^{-1}$) |
|---|---|---|---|
| REBaCuO bulk | 100 | 0.33 | $5.20 \times 10^{-6}$ |
| Al alloy | 78 | 0.34 | $1.48 \times 10^{-5}$ |

($E$: Young's modulus, $\nu$: Poisson ratio, $\alpha_0$: thermal expansion coefficient)

## 3. Numerical simulation results and discussion

### *3.1. Electromagnetic hoop stress, $\sigma_\theta^{mag}$*

Figure 2(a) shows final trapped field, $B_t(t = 7\ s)$, at the centre of the ring-shaped bulk with the "Ring" reinforcement ($r = z = 0$ mm), as a function of the applied pulsed field, $B_{ex}$, at $T_s$ = 65, 45 and 25 K. The $B_t$ value increases moderately with increasing $B_{ex}$, takes a maximum of 1.07 T at $B_{ex}^*$ = 2.5 T at 65 K, and then subsequently decreases. We define the activation field as $B_{ex}^*$, at which the bulk achieved the maximum trapped field, $B_{t,max}$. The $B_{ex}^*$ and $B_{t,max}$ values increased with decreasing $T_s$, which originates from the enhancement of $J_c$ at lower temperatures and subsequent increased Lorentz force. It is therefore harder for magnetic flux to penetrate into centre of the bulk at lower $T_s$. Figure 2(b) shows maximum temperature rise, $\Delta T_{max}$, of the outer surface of the bulk ($r$ = 30 mm, $z$ = 0 mm), as a function of $B_{ex}$ at $T_s$ = 65, 45 and 25 K. $\Delta T_{max}$ increased with increasing $B_{ex}$ and with lowering $T_s$ for all cases due to the increase of the dynamical motion of the magnetic flux against the vortex pinning force, $F_p$, and the viscous force, $F_v$, and also due to the lowering the specific heat for the bulk [19].

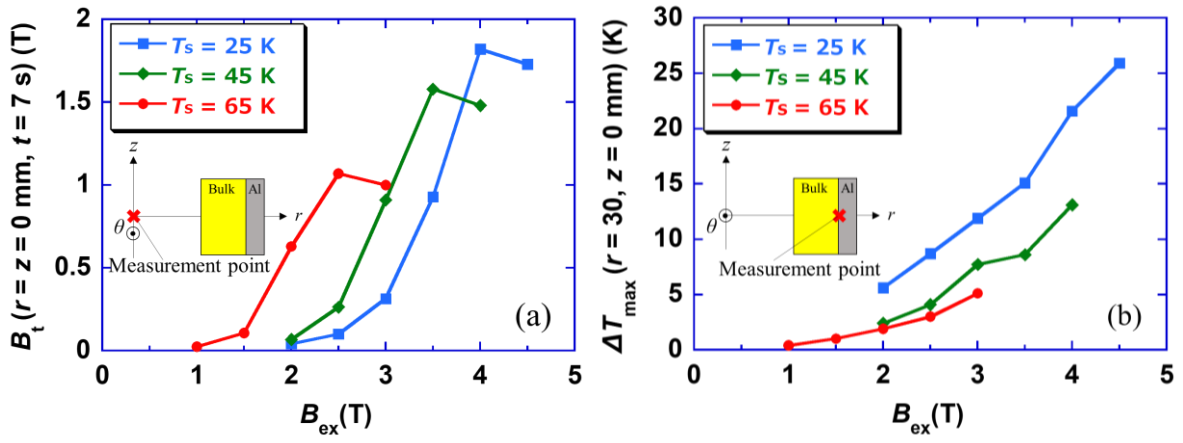


**Figure 2.** (a) Final trapped field, $B_t(t = 7$ s), at the centre of the bulk ($r = z = 0$ mm) and (b) maximum temperature rise, $\Delta T_{max}$, of the outer surface of the bulk ($r = 30$ mm, $z = 0$ mm), as a function of the applied pulsed field, $B_{ex}$, at $T_s$ of 65, 45 and 25 K for the ring-shaped bulk with the "Ring" reinforcement.

Figure 3(a) shows maximum electromagnetic compressive hoop stress, $\sigma_\theta{}^{mag}{}_{max}$, in the ascending stage, at the inner surface of the ring-shaped bulk ($r$ = 18 mm, z = 0 mm) with the "Ring" reinforcement, as a function of $B_{ex}$ at $T_s$ = 65, 45 and 25 K. The compressive $\sigma_\theta{}^{mag}{}_{max}$ value gradually increases with increasing $B_{ex}$ and approaches a constant value when $B_{ex}$ overcomes the magnetic shielding. The compressive $\sigma_\theta{}^{mag}{}_{max}$ also increases at lower $T_s$, which again originates from the enhancement of $J_c$ at lower temperatures and subsequent increased Lorentz force. The maximum electromagnetic tensile hoop stress, $\sigma_\theta{}^{mag}{}_{max}$, in the descending stage is also shown in Fig. 3(b), which is about half of the maximum compressive stress. During FCM, the electromagnetic tensile stress develops in the bulk, in which the mechanical fracture sometimes happens in the case that the tensile stress is larger than the fracture strength of the bulk [20 - 22]. On the other hand, not only a tensile stress, but also a compressive stress develops during PFM. The fracture strength of REBaCuO bulks under compressive stress has been reported to be several times larger than that under tensile stress [23, 24]. However, the stress distribution in the ring-shaped bulk is different from that in the disk-shaped bulk. Since the stress concentration occurs around the bore of a ring-shaped bulk, the stress increases locally. The risk of fracture where this stress concentration occurs also increases with decreasing width of the ring-shaped bulk. It is, therefore, necessary to reinforce the ring-shaped bulk for the compressive stress as well as tensile stress during PFM.

Figure 4 shows time evolution of the electromagnetic hoop stress, $\sigma_\theta{}^{mag}(t)$, at the inner surface of the ring-shaped bulk ($r$ = 18 mm, z = 0 mm), for various reinforcement structures for $B_{ex}$ = 4.0 T at $T_s$ = 25 K. The time evolution of the applied pulsed field, $B_{ex}(t)$, is also shown. Increasing the applied field, $\sigma_\theta{}^{mag}$ starts to increase negatively (compressive) and takes a peak value of -32.2 MPa at $t$ = 9 ms for the ring-shaped bulk with the "Ring" reinforcement. After that, $\sigma_\theta{}^{mag}$ increases positively, and changes to a tensile stress of +6.5 MPa at $t$ = 40 ms, which result from the change of the direction of the induced superconducting current. The maximum compressive $\sigma_\theta{}^{mag}{}_{max}$ was reduced for the other reinforcement structures, corresponding to approximately 67% (-21.5 MPa) for the "Cap Cover", 65% (-20.9 MPa) for the "Full Cover" and 54% (-17.4 MPa) for the "Full Cover wide", compared to that for the "Ring" reinforcement. The improved reinforcement structures, including the inner ring were more effective to reduce the compressive stress for the ring-shaped bulk during PFM.

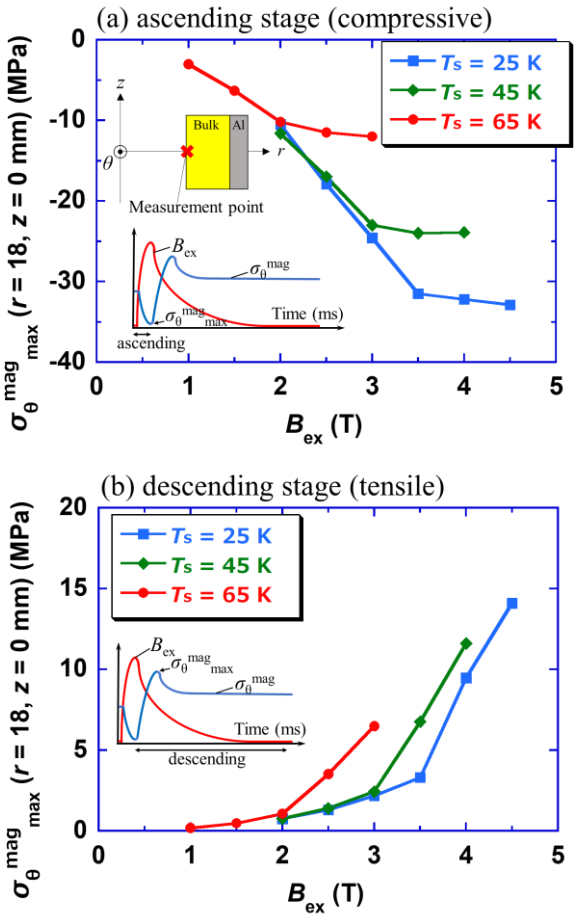


**Figure 3**. Maximum electromagnetic (a) compressive stress in the ascending stage and (b) tensile stress, $\sigma_\theta^{mag}{}_{,max}$, in the descending stage at the inner surface of the bulk ($r$ = 18 mm, $z$ = 0 mm) of the ring-shaped bulk with the "Ring" reinforcement, as a function of $B_{ex}$ at $T_s$ = 65, 45 and 25 K.

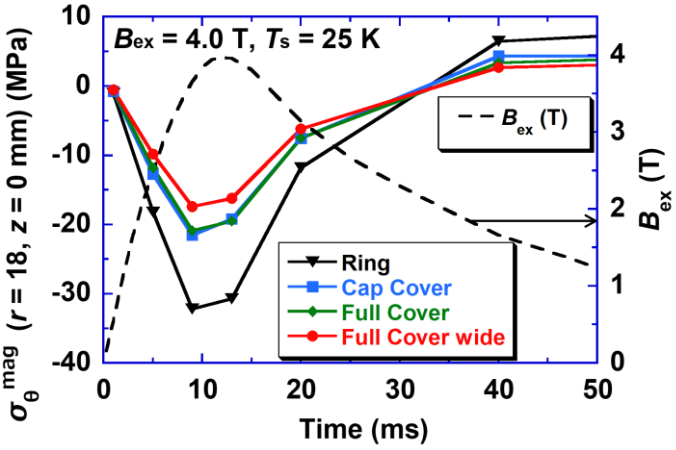


**Figure 4**. Time evolution of the electromagnetic hoop stress, $\sigma_\theta^{mag}$, at the inner surface of the ring-shaped bulk ($r$ = 18 mm, $z$ = 0 mm) for the various reinforcement structures for $B_{ex}$ = 4.0 T and at $T_s$ = 25 K.

Figure 5 shows contour maps of the electromagnetic hoop stress, $\sigma_\theta^{mag}$, during PFM ($B_{ex}$ = 4.0 T, $T_s$ = 25 K, $t$ = 9 ms, reaches maximum compressive stress) for the ring-shaped bulk with the various reinforcement structures. Here, the $\sigma_\theta^{mag}$ value was the maximum at the inner periphery of the ring-shaped bulk. The results clearly indicated that the highest electromagnetic compressive stress develops in the bulk with the "Ring" reinforcement. In the case of the "Cap Cover", as shown in Fig. 5(b), the reinforcement at the bottom of the bulk is not enough, compared to those of the bulks with the "Full Cover" in Fig. 5(c) and with the "Full Cover wide" in Fig. 5(d).

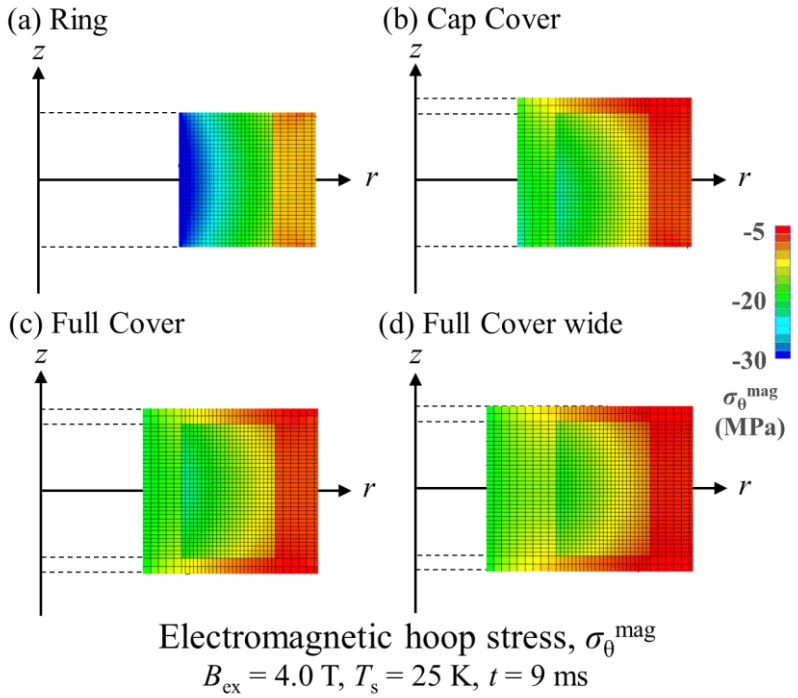


**Figure 5**. Contour maps of the electromagnetic hoop stress, $\sigma_\theta^{mag}$, during PFM ($B_{ex}$ = 4.0 T, $T_s$ = 25 K, $t$ = 9 ms) for the ring-shaped bulk with the various reinforcement structures.

### *3.2. Thermal hoop stress, $\sigma_\theta^{therm}$*

During PFM, a large temperature rise occurs in the bulk, compared with that during FCM [25]. The inhomogeneous temperature distribution results in a thermal stress due to the inhomogeneous thermal displacement in the bulk. Figure 6 shows the contour map of the temperature during PFM ($B_{ex}$ = 4.0 T, $T_s$ = 25 K, $t$ = 11 ms, reaches maximum tensile stress) for the various reinforcement structures. In Fig. 6(a), for the "Ring" reinforcement, the temperature rise mainly takes place at the outer periphery of the ring-shaped bulk, which resulted in a temperature as high as 45 K. The temperature rise decreased slightly for the bulk for the other reinforcement structures due to heat diffuse to the Al alloy holder.

Figure 7 shows the contour maps of the thermal hoop stress, $\sigma_\theta^{therm}$, during PFM ($B_{ex}$ = 4.0 T, $T_s$ = 25 K, $t$ = 11 ms) for the various reinforcement structures. The inhomogeneous temperature distribution results in a thermal stress. In Fig. 7(a) for the "Ring" reinforcement, the compressive stress develops at the narrow region of the outer periphery of the ring-shaped bulk, which was as small as -8 MPa. Although the bulk periphery thermally expands along the $r$-direction due to the large temperature rise, as shown in Fig. 6(a), the Al alloy ring cannot expand due to the small temperature rise. As a result, a thermal compressive stress develops in the outer region of the ring-shaped bulk and a thermal tensile stress develops in the inner region of the ring-shaped bulk. For the other reinforcement structures, as shown in Figs. 7(b) – 7(d), the thermal tensile stress can be reduced, compared to the "Ring" reinforcement. On the other hand, the thermal compressive stress, $\sigma_\theta^{therm}$, increases for the improved

reinforcement structures. However, the thermal compressive stress, $\sigma_\theta^{therm}$, in the bulk is much smaller than the electromagnetic compressive stress, $\sigma_\theta^{mag}$, and the region where the compressive stress is maximum is different. These results suggest that the influence of the thermal stress is relatively small.

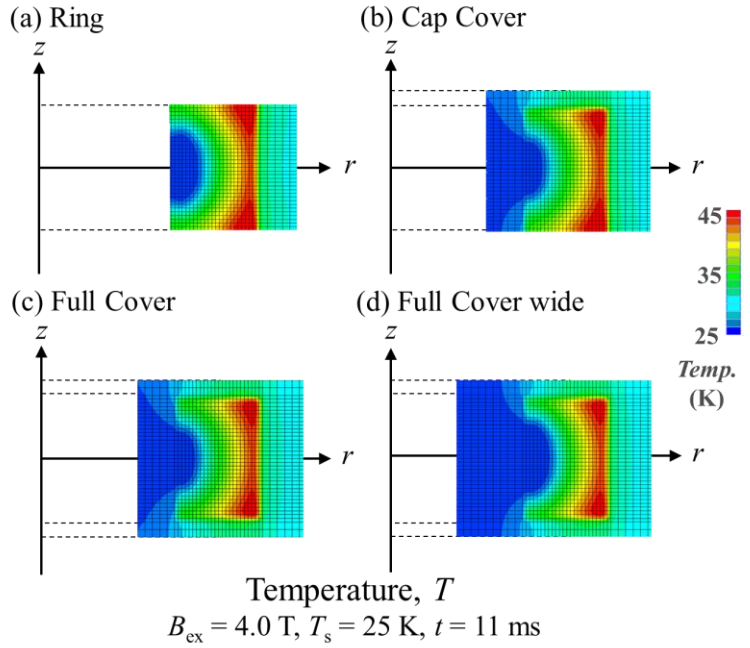


**Figure 6**. Contour maps of the temperature during PFM ($B_{ex}$ = 4.0 T, $T_s$ = 25 K, $t$ = 11 ms) for the various reinforcement structures.

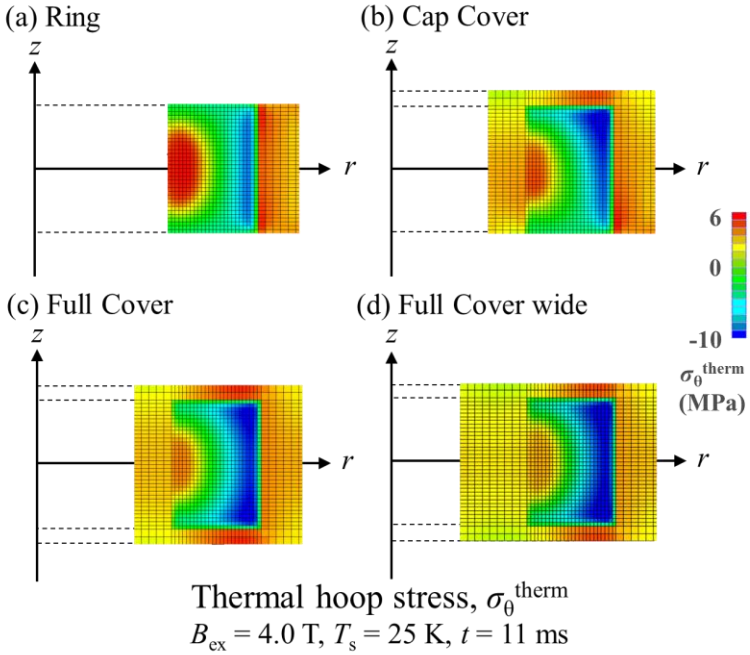


**Figure 7**. Contour maps of the thermal hoop stress, $\sigma_\theta^{therm}$, during PFM ($B_{ex}$ = 4.0 T, $T_s$ = 25 K, $t$ = 11 ms) for the various reinforcement structures.

*3.3. Comparison to disk-shaped bulk.*

Finally, we compare the electromagnetic hoop stress, $\sigma_\theta^{mag}$, of the ring-shaped bulk with that of the disk-shaped bulk during PFM. Figure 8 shows the electromagnetic hoop stress, $\sigma_\theta^{mag}$, for the ascending stage of PFM ($B_{ex}$ = 4.0 T, $T_s$ = 25 K, $t \leq$ 13 ms) for the disk-shaped bulk (60 mm in O.D. and 17 mm in H) as shown in Fig. 8(c), compared to the ring-shaped bulk, as shown in Fig. 1(a). The disk-shaped bulk is also mounted in an Al alloy ring holder 5 mm in width. The compressive stress takes a maximum of -32.2 MPa at the inner periphery of the ring-shaped bulk, as shown in Fig. 4. On the other hand, in the case of the disk-shaped bulk of the same O.D., a smaller compressive stress takes a maximum of -16.9 MPa in the bulk. Wu *et al.* described the maximum compressive hoop stress of the disk-shaped bulk (46 mm in O. D. and 15 mm in H) during PFM ($B_{ex}$ = 6.25 T, $T_s$ = 30 K) was -25.5 MPa [10]. The difference of the compressive stress values results mainly from the $B_{ex}$ value, because the compressive stress increases with increasing $B_{ex}$. These results indicate that the disk-shaped bulk is tough and is less likely to break during PFM, compared with the ring-shaped bulk, even if the applied pulse field is stronger and the operating temperature is lower.

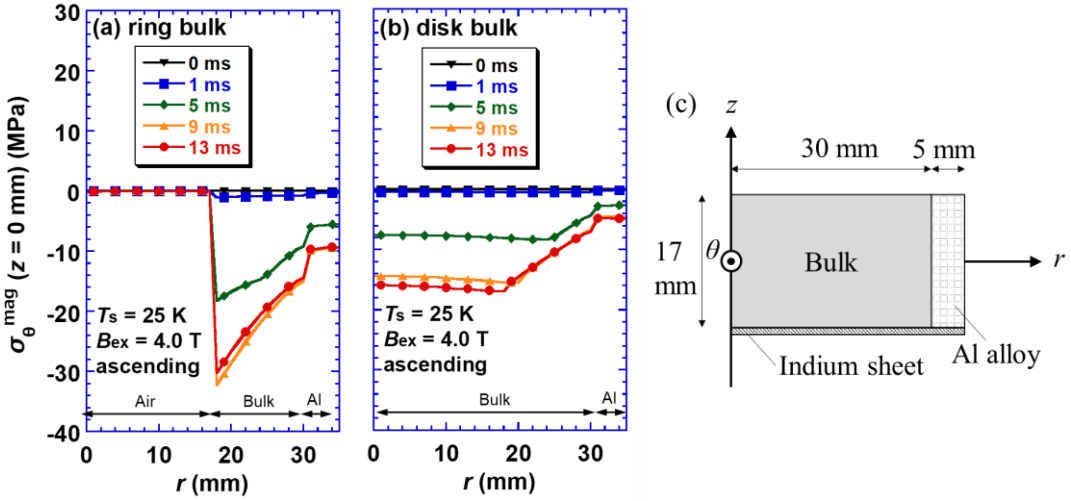


**Figure 8**. The electromagnetic hoop stress, $\sigma_\theta^{mag}$, for the ascending stage of PFM ($B_{ex}$ = 4.0 T, $T_s$ = 25 K, $t \leq$ 13 ms) for the (a) ring-shaped bulk and (b) disk-shaped bulk (60 mm in O.D. and 17 mm in H), each of which were reinforced by an Al alloy ring 5 mm in width and (c) schematic view of numerical model for disk-shaped bulk.

## 4. Conclusion

We have performed numerical simulations of the electromagnetic, thermal and mechanical properties of REBaCuO ring-shaped bulk with various reinforcement structures during PFM. Compressive and tensile electromagnetic stresses, $\sigma_\theta^{mag}$, develop in the ring-shaped bulk during the ascending and descending stages of PFM, respectively. These stresses increased with lower operating temperatures and higher applied fields. In particular, in order to reduce the compressive stress, the fully encapsulated reinforcement was optimal, which can achieve the lowest electromagnetic compressive stress and corresponds to about 54% of that for the conventional ring reinforcement structure. Compared with the disk-shaped bulk, the ring-shaped bulk with the "Ring" reinforcement has a risk to break by the electromagnetic compressive stress during the ascending stage during PFM. As such, suitable reinforcement must be considered.

**Acknowledgements**
This research is partially supported from JSPS KAKENHI Grant No. 15K04646. M. D. Ainslie would like to acknowledge financial support from an Engineering and Physical Sciences Research Council (EPSRC) Early Career Fellowship EP/P020313/1. All data are provided in full in the results section of this paper.

**References**

[1] Nakamura T, Tamada D, Yanagi Y, Itoh Y, Nemoto T, Utsumi H and Kose K 2015 *J. Magn. Reson*. **259** 68–75
[2] Zhou D, Izumi M, Miki M, Felder B, Ida T and Kitano M 2012 *Supercond. Sci. Technol.* **25** 103001.
[3] Tomita M and Murakami M 2001 *Physica C* **354** 358–362
[4] Fujishiro H, Ainslie M D, Takahashi K, Naito T, Yanagi Y, Itoh Y and Nakamura T 2017 *Supercond. Sci. Technol.* **30** 085008
[5] Takahashi K, Fujishiro H, Naito T, Yanagi Y, Itoh Y and Nakamura T 2017 *Supercond. Sci. Technol.* **30** 115006
[6] Fujishiro H, Naito T, Yanagi Y, Itoh Y and Nakamura T 2019 *Supercond. Sci. Technol.* **32** 065001
[7] Fujishiro H, Naito T and Awaji S 2019 *Supercond. Sci. Technol.* **32** 045005
[8] Ainslie M D, Huang K Y, Fujishiro H, Chaddock J, Takahashi K, Namba S, Cardwell D A and Durrell J H 2019 *Supercond. Sci. Technol.* **32** 034002
[9] Yang X, Li X, He Y, Wang X and Xu B 2017 *Physica C* **535** 1-8
[10] Wu H, Yong H and Zhou Y 2018 *Supercond. Sci. Technol.* **31** 045008
[11] Johansen T H, Wang C, Chen Q Y and Chu W -K 2000 *J. Appl. Phys.* **88** 2730–2733
[12] Johansen T H 2000 *Supercond. Sci. Technol.* **13** R121
[13] Johansen T H 1999 *Phys. Rev. B* **60** 9690
[14] Shimoyashiki F, Fujishiro H, Hirano T, Naito T and Ainslie M D submitted to *J. Phys.: Conf. Ser.*
[15] Mochizuki H, Fujishiro H, Naito T, Itoh Y, Yanagi Y and Nakamura T 2016 *IEEE Trans. Appl. Supercond*. **26** 6800205
[16] Fujishiro H and Naito T 2010 *Supercond. Sci. Technol*. **23** 105021
[17] Ainslie M D and Fujishiro H 2015 *Supercond. Sci. Technol.* **28** 053002
[18] Kim Y B, Hempstead C F and Stmad A R 1965 *Phys. Rev.* **139** A1163
[19] Yokoyama K, Kaneyama M, Fujishiro H, Oka T and Noto K 2005 *Physica C* **426-431** 671-675
[20] Lee D and Salama K 1990 *Japan. J. Appl. Phys.* **29** L2017
[21] Nariki S, Sakai N, Tomita M and Murakami M 2002 *Physica C* **378-381** 779–782
[22] Katagiri K, Murakami A, Kan R, Kasaba K, Noto K, Muralidhar M, Sakai N and Murakami M 2003 *Physica C* **392–396** 526–530
[23] Kan R, Katagiri K, Murakami A, Kasaba K, Shoji Y, Noto K, Sakai N and Murakami M 2004 *IEEE Trans. Appl. Supercond*. **14** 8132078
[24] Murakami A, Katagiri K, Kan R, Miyata H, Shoji Y, Noto K, Iwamoto A and Mito T 2005 *Physica C* **426–431** 644–648
[25] Fujishiro H, Oka T, Yokoyama K, Kaneyama M and Noto K 2004 *IEEE Trans. Appl. Supercond*. **14** 8132063